Research Article

# Modeling dynamic mechanical system behavior using sequence modeling of embodiment function relations: case study on a hammer mechanism

**Andreas Wettstein**[1] · **Patric Grauberger**[1] · **Sven Matthiesen**[1]

Received: 29 November 2019 / Accepted: 4 January 2021 / Published online: 12 January 2021

**Abstract**
In engineering design, an issue for using complex simulation models in system analysis are unknown causes for dynamic system behavior, which make parameterization difficult. This paper presents a case study in which a structured system analysis is used for the parameterization of complex dynamic multi-domain models. The dynamic system behavior of an impact wrench during fastening of a bolt is analyzed and modeled using the Contact and Channel Approach for structured parameterization of a multibody simulation model. This qualitative model building serves as a basis for a simulation model that quantifies the relations of design parameters and system behavior. Comparison with experimental test results is done as a validation. With this approach, the behavior identified in the simulation model could be traced back in a structured way to its cause in the system embodiment. The simulation model represented the real dynamic system behavior with an initial sufficient precision, but showed a lack of precision in detail. On this basis, the Contact and Channel Model was extended by adding additional statistical behavior of the system. Parameters of the system embodiment were identified qualitatively to improve the simulation model. A limitation in qualitative modeling of dynamic changes in the system has been identified that needs to be addressed in further research.

**Keywords** Modeling · Validation · Engineering design · Impact wrench · Parameter identification

## 1 Introduction

In engineering design, modeling of the dynamic behavior of a product or its subsystems is often necessary to understand and then optimize the product. Recent mechatronic products often are very complex. Therefore, it takes much effort in time and cost to develop models, which represent the product's dynamic behavior. Modeling languages like Simscape™ or Modelica® are commonly used to conveniently model complex physical systems throughout various domains as lumped-parameter models. These quantitative models usually rely on the system structure and on the experience of design engineers. This experience consists of knowledge on how a system works, i.e. how its embodiment is linked to its behavior and functions. On a structural level, this is known as product architecture. For example, the functions of components in a hammer drill are modeled in its product architecture. The gearbox transmits torque and rotational speed, the hammer mechanism creates the impact, and so on. Identification of the cause for a certain characteristics of the impact is not in focus of the product architecture model. This detailed embodiment function relation (EFR) is difficult to capture, as it describes the connection between the specific products' embodiment (including known and unknown parameters) and its abstract functions (including behavior). For example, it is unclear why the torque of the impact wrench has a large

---

✉ Patric Grauberger, Patric.grauberger@kit.edu; Andreas Wettstein, Andreas.wettstein@kit.edu; Sven Matthiesen, Sven.matthiesen@kit.edu | [1]Karlsruhe Institute of Technology (KIT), IPEK–Institute of Product Engineering, Karlsruhe, Germany.

SN Applied Sciences (2021) 3:128 | https://doi.org/10.1007/s42452-021-04149-8

scatter. Details of the embodiment causing this behavior can be identified when modeling the EFRs.

Besides being present in the mind of the design engineer, this knowledge about EFRs can also be explicated into models. Design engineers can use a multitude of these models, e.g. already existing simulation models, experimental data, and other documentations of the design, as a basis for quantitative models. Besides, many assumptions regarding the relevance of embodiment parameters have to be made. During parameter identification, the model behavior is fitted to the real system behavior. The relation of model parameters and model behavior could be observed during that process and could be reflected onto the EFRs used to develop the model. Erroneous assumptions regarding EFRs, which could obstruct product development processes, might be discovered using a modeling approach which connects qualitative and quantitative models.

The challenge in developing dynamic systems like impact wrenches is that the complex system behavior makes assumptions necessary. Design engineers need to investigate this behavior and understand its relation to embodiment parameters in order to synthesize an optimized system. Therefore, erroneous assumptions regarding EFRs need to be avoided.

The aim of this contribution is to utilize a new approach, which uses EFRs during parameter identification and reflects results onto them, in a case study. The aim of the case study is to develop and parameterize a dynamic model of an impact wrench hammer mechanism using a structured modeling approach for EFRs. This is accomplished by using qualitative sequence modeling with the Contact and Channel Approach (C&C$^2$-Approach). Additionally, the developed hammer mechanism model is coupled to a state-of-the art bolted-joint model, which is assumed to have a significant influence on the hammer mechanism behavior. From this, the system- specific challenge of coupling simulation models of the impact wrench and the bolted joint emerges.

The paper is structured as follows: An overview of literature on existing modelling approaches for EFRs and a description of the system under investigation for the case study are given. Then, the approach chosen in the case study is described and finally, the results gained by following this approach in investigation of the dynamic system are shown.

### 1.1 Review of literature–modeling EFRs in dynamic systems

Handling EFRs is important to design engineers, as they need to define an embodiment of a technical system to realize its desired functions. Modeling methods that contain elements to describe EFRs have been developed to support engineering design. Axiomatic Design [1] or the Function Behavior Structure (FBS) framework [2] are used to describe design processes and contain elements to describe entities and relations of technical systems. They focus on understanding and modeling design processes, while their support in modeling EFRs is limited.

Characteristics Properties Modelling (CPM) comprises elements to describe the characteristics and properties of a product [3, 4]. It focuses on the structuring of these elements to support product developers in handling them in complex products. With CPM, the modeling of EFRs is possible, however, its support in the analysis of unknown EFRs is limited, as it relies on defined parameters of the products' embodiment. A visualization, which can support in problem solving tasks [5], is not integrated. The domain theory [6] contains visualization aspects for explicit modeling of embodiment parts and their relation to functions in the 'organ domain' and describes the relevant models. All of these described modeling methods in engineering design lack support in the modeling of EFRs in quasi-static or dynamic systems. These systems change the physical configuration of their embodiment during operation. This does not hinder modeling of the product architecture. However, in the technical details, it gets difficult to identify which EFRs are active at a certain state[1] of the system. To gain knowledge about EFRs in the analysis of quasi-static and dynamic systems, the differentiation of their behaviors into states can be a reasonable approach.

Bond graphs provide a formalized description of EFRs in technical systems and are able to model dynamic systems. They allow the handling of complicated interactions, however, their possibilities to visualize the defined shape and its interaction during function fulfillment in a realistic representation are limited. Contact surfaces and their connections remain schematic in the graph model. This is why they reach their limits in the analysis of dynamic systems in which non-standardized elements are used.

Modeling of state changes in design is established in the area of functional modeling, where many approaches use graph-based state descriptions on a functional level. The entity relationship model [7] or the state charts [8] describe states as sets of parameters of objects that can change in transition to a new state. Models based on them, like the system state flow diagram [9] enable the building of powerful models containing different energy flows through the system. The integrated function modeling

---

[1] In this context, a state means a fixed physical configuration of a technical system during a certain timespan. These states can change in a fixed sequence or due to trigger events. They can be divided into sub-states if a more detailed modeling is necessary.

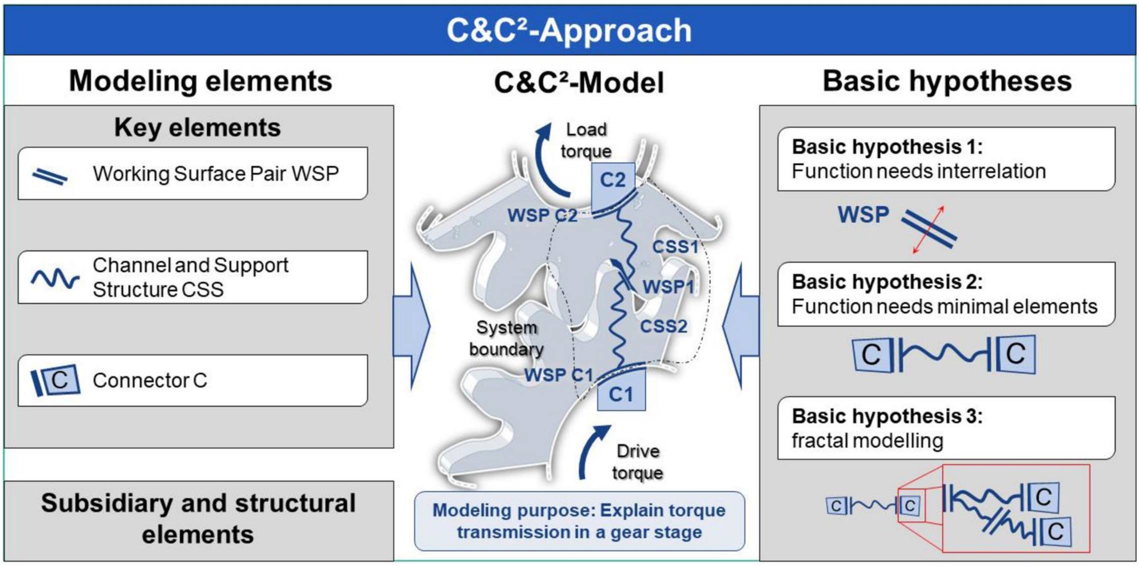

**Fig. 1** The C&C$^2$-Approach, according to [13]

framework IFM [10] enables different views on process flow, interactions, states, and effects with the possibility to add even more. The approach by Mokhtarian et al. [11] combines functional modeling with physical models based on the bond graph theory. This approach enables the description of EFRs and consideration of states through state variables. These modeling methods help to depict and structure a system with focus on its functionality. Powerful function models can be created with them, and partially, a relation to the details in embodiment is also possible. However, the influence of the details of the embodiment has to be known before they can be modeled (e.g. the influence of the system variable *nozzle diameter* of a glue gun on the glue gun flow). In this case, the EFR is clear. However, in systems, where dynamic effects influence the behavior (e.g. in which way the anvil diameter in the hammer drill influences the torque scatter), this becomes more difficult. Therefore, difficulties emerge in using functional modeling approaches in identifying EFRs in the analysis of dynamic system behavior.

## 1.2 The contact and channel approach for qualitative and visual modeling of EFRs

The C&C$^2$-Approach [12–14] is a modeling method that focuses on a state-differentiated modeling of EFRs and uses the principle of visualization combined with structured elements. It has been developed to support product developers with a thinking tool for modeling of EFRs in static and quasi-static systems. The key elements provided allow the explication of EFRs and therefore can be used to express ideas, assumptions, and insights in explicit visual models (compare Fig. 1). In a previous case study, the C&C$^2$-Approach has been used for building a multibody simulation model [13] Here, it supported design engineers in structuring of information and in using different model domains for solving a design problem. The approach is used in this study as well and thus is explained in more detail in the following.

Spatial and temporal system boundaries are defined, where only parts of the system are investigated, or, where specific periods of time during function fulfillment (states) are investigated. Based on visualizations of the systems' embodiment, e.g. a sketch of the system, a CAD cross-section, or a photo of a real system, EFRs are derived within the set boundaries. The levels of detail of the used visualizations have to be sufficient to allow the explicit expression of the EFRs. The key elements of the C&C$^2$-Approach, the Working Surface Pair (WSP), the Channel and Support Structure (CSS) and the Connector (C) are used to create representations of the EFRs. WSPs are created when two arbitrary surfaces get into contact and transmit energy, material, or information. The CSS connects two WSPs and transports energy, material, or information. The C comprises the effects of system parts outside the boundaries and represents the system's environment.

These elements are shown in Fig. 1 (left side). The initial C&C$^2$-Model is completed by assigning parameters to the key elements. More detailed models can be derived if necessary, or the system boundaries can be shifted to investigate other parts of the system using this initial C&C$^2$-Model. Also, the basic hypotheses for the modeling approach are shown in Fig. 1 (right side).

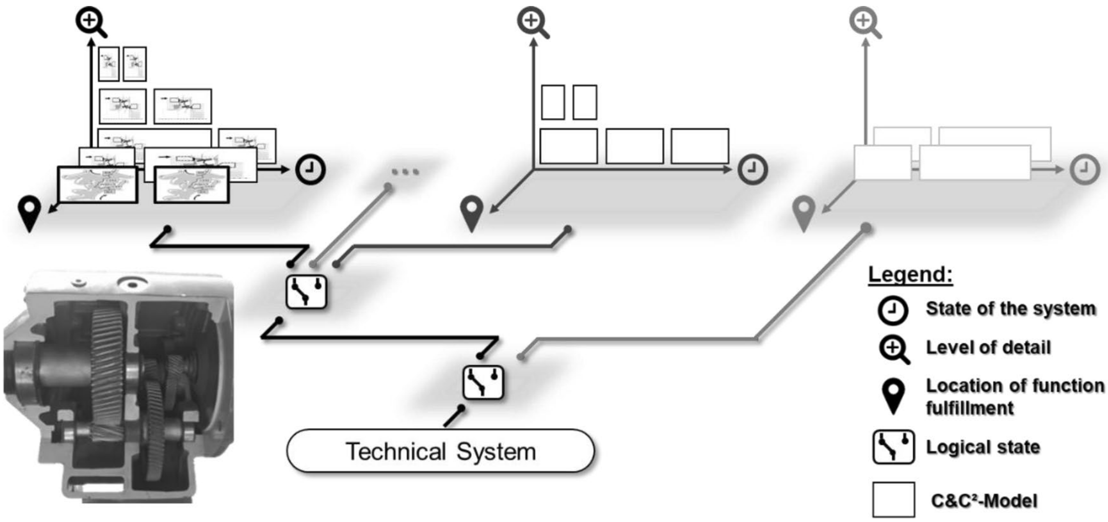

**Fig. 2** Overview of the C&C$^2$-Sequence model [15]

When a system changes its configuration (quasi-static or dynamic), the static C&C$^2$-Model is no longer valid, as WSPs, CSSs or Connectors emerge, disband or change their properties. A new C&C$^2$-Model emerges, which can be connected to the existing ones representing a state and forming a C&C$^2$-Sequence model with the other state models. The C&C$^2$-Sequence model in its current development contains four dimensions, in which a system can change its configuration [15] An overview is shown in Fig. 2.

Here, the visualization of the dimensions *state of the system*, *level of detail*, and *location of function fulfillment* is made in a three-dimensional coordinate system. The dimension *state of the system* describes state changes over time that happen when the system runs in a sequence, e.g. the teeth of a gear that change states in a fixed sequence of the rotation of the gear. The dimension *level of detail* enables the structuring of analytical models with a different focus, an example being an overview model of the force flow and a detailed model of the interaction of two gear teeth. The dimension *location of function fulfillment* describes different locations, in which effects occur that influence the systems behavior. Differentiating in this dimension is similar to dividing a system into different subsystems, for example the bearing of the input shaft and output shaft of the gearbox. The fourth dimension *logical state* differentiates state changes caused by certain triggers, for example when a gearbox is shifted from first to second gear. It is visualized through triggers that lead to different three-dimensional coordinate systems, as four-dimensional coordinate systems are difficult to visualize, which is important in using the C&C$^2$-Approach [15] An initial investigation of dynamic system behavior using the C&C$^2$-Sequence model has been conducted to identify unknown system behavior of an impact wrench [16].

To verify the built-up models, hypotheses can be derived from identified parameters of the systems embodiment and its behavior. They can follow the principles of hypotheses for damage analysis [17] and orientating tests [18], where focused simplification of a system is done to gain knowledge about EFRs.

### 1.3 Investigating a dynamic system-working principle of impact wrenches

Impact wrenches are used when high torque is demanded in applications that require hand-held power tools, for example in steel construction or in repair shops. For applications where bolts are loosened, the impact wrench is commonly used because of its advantages in terms of speed and user's exertion. In applications where tightening of bolts is necessary, there are issues regarding the precision of the resulting clamping force. The torque of an impact wrench develops dynamically and therefore strongly depends on the interactions with the system environment. This means that different bolted joints and also different use cases or users greatly influence the resulting preload force [19]. Even in the process of tightening a bolt, with increasing the preload in the bolted connection, the effective stiffness rises and the amplitude of the impact torque rises, too [20]. It is difficult to draw up formulas and tables showing the interrelationships. Therefore, impact wrenches are not allowed to be used in most applications or are provided with a high safety factor like in VDI 2230 [21]. This is caused by the lack of a flexible as well as precise control method for impact wrenches [22]. A common approach nowadays is the model-based control of tightening systems. Therefore, an analysis of the impact wrenches for modeling

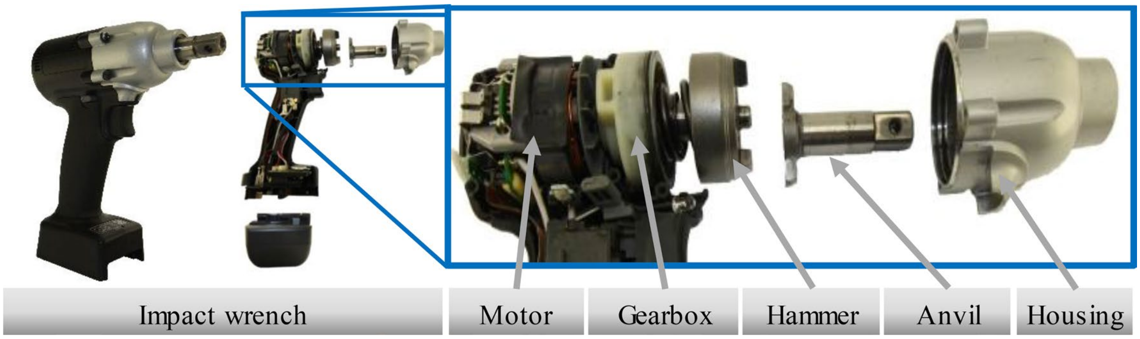

**Fig. 3** Subsystems in the impact wrench [16]

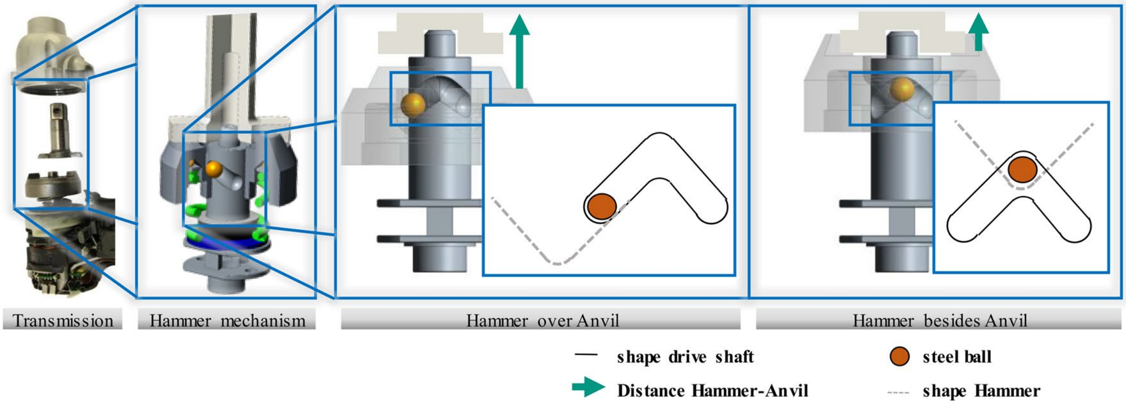

**Fig. 4** V-shaped tracks of the hammer mechanism [16]

the system can be the basis for the development of future control methods for the tightening process with impact wrenches.

The main advantage of impact wrenches over cordless screwdrivers and other continuous power tools is the low exertion by the user while applying high torque on bolting applications. This is done by using a rotational hammer mechanism where the hammer's moment of inertia supplies the energy for the torque development. The hammer mechanism and the components around hammer and anvil are shown in Fig. 3.

The motor accelerates a hammer mass, almost with a constant torque, which hits the anvil and thereby generates a torque pulse. The torque pulses generated in this way are significantly greater than the torque of the motor and very short (pulse duration less than 0.5 ms). The drive shaft has two opposing v-shaped grooves with a semicircular cross-section on the outer surface, in which two steel balls are located. The hammer, which also has two mirrored internal V-shaped groove tracks on the inside, is mounted on the drive shaft and connected with it by the two steel balls. The interaction of hammer and drive shaft is shown in Fig. 4.

The rotation of the hammer is coupled with the axial movement of the hammer with respect to the drive shaft by the balls following the grooves on both parts. Additionally, a preloaded spring, which also stores energy, is mounted between the transmission and the hammer.

### 1.4 Dynamic models of impact wrenches and bolted joints

For the development of new hammer mechanisms for impact wrenches, detailed knowledge about the interactions as well as dynamic simulation models are required. In particular, these models can be used for drive train design or for the development of tightening methods. To derive such system models, it is necessary to take into account all interacting subsystems. These subsystems, for example those of an impact wrench, are shown in Fig. 5 [23].

The interactions between the subsystems are particularly important in the development of complex dynamic models, because of the time dependencies and nonlinearities and their direct influence on the working result.

Sieling based his model derivation on an energy balance of the single impacts in accordance with the classical

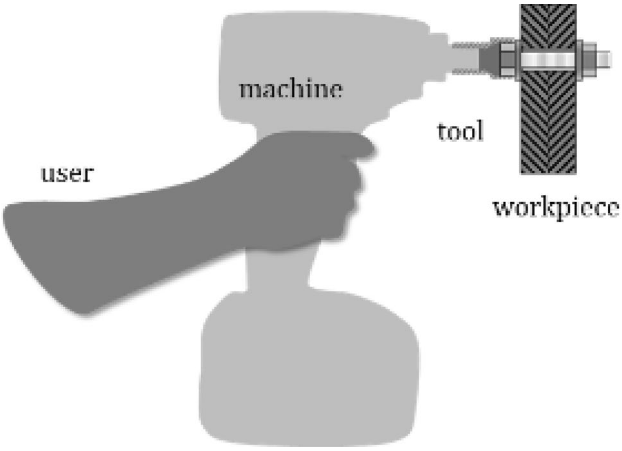

**Fig. 5** Impact wrench in interaction with user and workpiece [23]

impact theory; the preload force of the bolted joint is defined as the main model objective value [20]. With the assumption of the course of the preload force as a geometric series, he derives a discrete formula for prediction of the preload force after a certain number of impacts [20]. A study regarding the energy consumption in impact tightening processes was conducted by Wallace [22].

Zhang and Tang show a lumped-parameter model of the hammer mechanism. For the parameterization of their model, a multi-objective optimization (MOO) approach is utilized while using measurement data of experiments with an impact mechanism and a hydraulic bolt tension calibrator. The resulting model is able to predict relevant states, and the maximum output torque and impact duration fit the experimental data well [24]. For bolted joints, lumped-parameter models also exist. One example is the lumped-parameter model for simulation of the dynamic tightening process developed by Japing et al. [25]. The objective of the model is to reproduce friction-induced rotational vibrations and to help understand the causes of the vibrations. The behavior of bolted joints depends on the tightening procedure [26]. The model by Japing et al. [25] is used in this paper as a basis and is being extended to take into account the actual test. Later on, the model is coupled with the hammer mechanism.

## 1.5 Case study

The objective of the case study is to develop a simulation model of a hammer mechanism and to couple this model successfully with a bolted-joint model. Because of its high dynamics, the hammer mechanism of an impact wrench is a suitable system for this case study.

Figure 6 shows the structure of the modeling approach. The approach is divided into three phases / steps. System structure modeling, parameterization, and model validation. The result of system structure modeling are a sequence model and a lumped-parameter model. The result of parameterization are quantified EFRs. In model validation, the quality of the lumped-parameter model is assessed against experimental data. The result of the modeling approach is a parameterized quantitative model, which is connected to the initial EFRs and quantifies them. In the following, the actions during the phases are explained in detail.

## 1.6 System structure modeling

At the beginning of the analysis, an initial understanding of the relations of the embodiment and system behavior of the impact wrench under investigation is needed as a basis for the modeling of the dynamic system. The HILTI SIW 22-A impact wrench was used in this case study. An initial static analysis of the components with the C&C$^2$-Approach is conducted and qualitative EFRs are derived. Based on these results and experimental data the temporal change

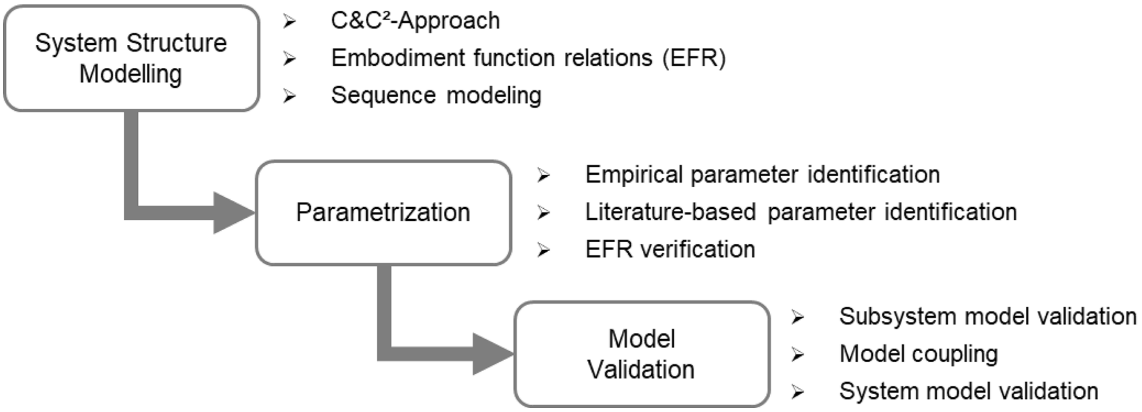

**Fig. 6** Modeling approach used in the case study

of the system is modelled as a C&C$^2$-Sequence model according to [13]. The model is then transferred into a lumped-parameter model in the Matlab® Simscape™ environment. The components are modeled as two lumped masses and a connecting spring and damper unit. Due to the overall high system stiffness, low masses and high dynamics, because of the impact, the differential system equations are stiff.

## 2 Parameterization

The geometric parameters as well as the stiffnesses and inertias are directly derived from the CAD model or corresponding FEM simulations. Damping coefficients, friction coefficient, and the contact coefficients for the impact need to be determined empirically. Therefore, experiments to measure the output torque are conducted. The test setup used is a torsional Hopkinson bar similar to the one employed in an arrangement by Espinosa et al. [27]. The original power tool was manipulated to allow preload force control by connecting it to the test rig. The tests were carried out with a fully charged battery. The power tool allows the user to choose between three power levels, i.e. slow, medium, and fast, corresponding with the rotational speed of the motor. The impact wrench is axially directly attached to the measurement shaft and set to the medium rotational speed (12,000 rpm motor speed). The strain gauges applied to the measurement shaft are connected to an amplifier (Honigmann Tensiotron® TS 621) and the measurement data is acquired using a DAQ at 50 kHz. Based on the C&C$^2$-Sequence model, the simulation model is derived and implemented in Simscape™ following the states defined in the C&C$^2$-Sequence model. The peak heights and peak durations are used as objective criteria for identification of the parameters for the simulation model. As starting values for the identification, parameter values of similar systems from the literature are used. Comparing the results of the simulation with the experimental result, deviations can be found which lead to an adjustment of the parameter values based on the C&C$^2$-Model and the corresponding EFRs. This means that if the simulated behavior deviates from the real behavior, the embodiment properties, which are supposed to define that behavior in reality, are adjusted in the simulation model. For example, if the computed peak height does not fit, the contact stiffness and damping might be adjusted. Adjustments in parameter values having the expected influence on the computed results are treated as indicators for verification of the underlying EFR. Adjustments that do not have the expected influence lead to a more thorough investigation of the underlying EFR. When the computed results sufficiently fit the measured data regarding the model purpose, the parameter identification is completed.

### 2.1 Model validation

In this case study, model validation is done in two main steps. The first step is the validation of the hammer mechanism model at a slow and fast rotational speed. Therefore, experiments with the setup described in Sect. 2.2 are performed at different rotational speeds (10’000 and 16’000 rpm motor speed) of the impact wrench. The experimental data is then compared to the computed data.

The second step is to couple the hammer mechanism model with the model of a bolted joint and to compare the simulation results with the experimental data. A second test setup as described in [28] is based on ISO 16,047 [29]. Figure 7 shows this test setup.

The basic principle of the test setup is the long torsional measuring bar, which allows precise measurement of torque impacts. Impacts are propagated as structure-borne sound waves along the measuring bar and are assessed completely before the reflected wave arrives [28]. The long torsional measuring bar is held by the clamping at the one end and at the other end, the bearing support is mounted. Decoupling of the thread and bearing friction is realized between these parts as shown in more detail in Fig. 8.

The impact wrench is depicted on the left. It is connected to the bolt head by a socket. A washer is mounted between the bolt head and torque support plate. Between this support and the nut, a needle bearing is mounted that allows a rotational degree of freedom. This means that there is a definite transmission of torque, so the bearing and thread torque are measured separately. The torque transmitted from the hexagonal bolt head via the washer to the plate is absorbed by four torque support arms, which allow an axial degree of freedom for the plate. The nut is inserted backlash-free into the torsional Hopkinson bar. The preload force is measured during tightening and loosening of the bolted joint with a strain-gauge-based force measuring ring (Manufacturer: HBM, Type: KMR/100kN). The thread friction torque is measured during tightening and loosening by a full bridge strain gauge arrangement on the torsional Hopkinson bar (Manufacturer: HBM, Type: CEA-06-062UV-350). The strain-gauge-based signals are amplified using a strain gauge amplifier (Manufacturer: Honigmann, Type: Tensiotron® TS 621 HD). The total torque is measured during manual loosening of the joint based on a full-bridge strain gauge arrangement as well. In the experiments, M10 8.8 bolts are used as lubricated by the manufacturer. The data is acquired at 150 kHz and filtered during post- processing with a Bessel filter of the 5th degree and a cut-off frequency of 20 kHz to reduce noise.

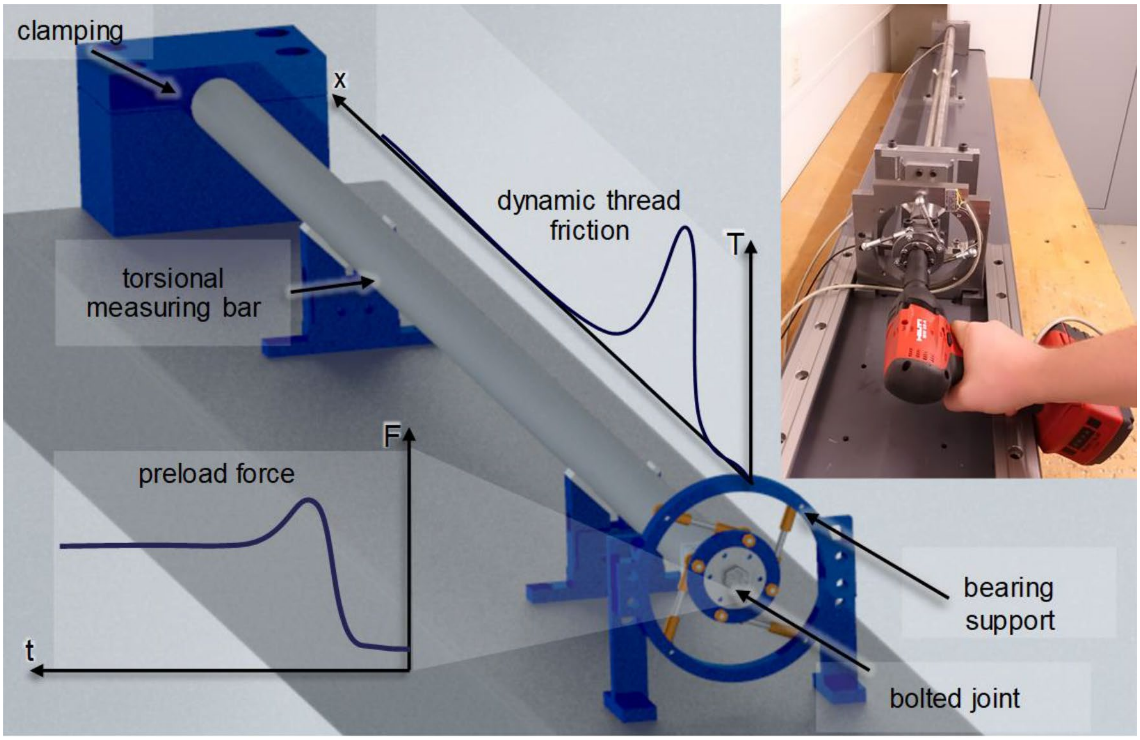

**Fig. 7** Test setup for measuring the dynamic thread friction and bolt preload force [30]

**Fig. 8** Decoupling of dynamic thread and bearing friction [28]

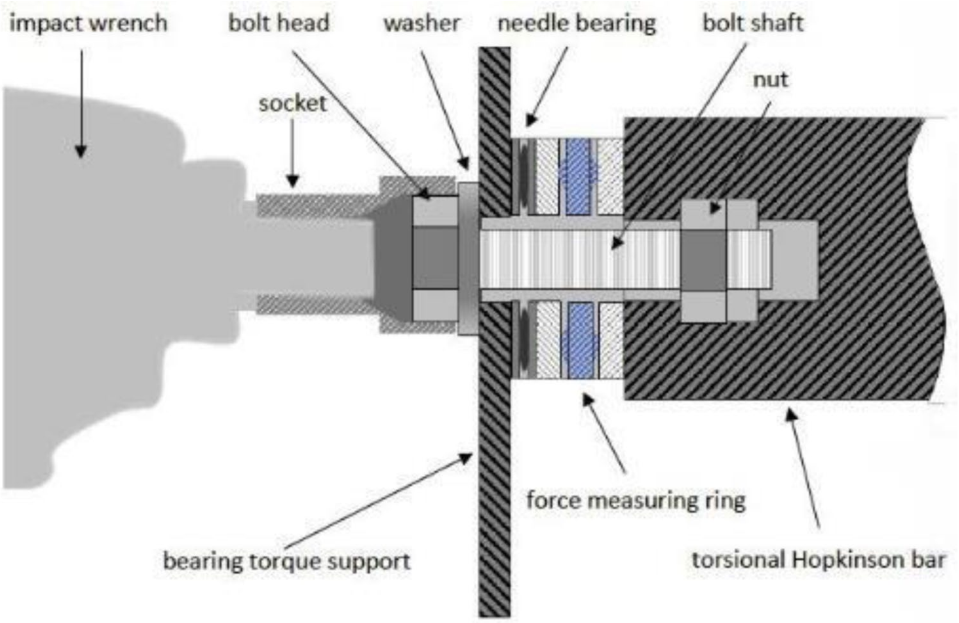

Based on the acquired data the coefficients of friction of the bolted joint are calculated and are used for the bolted joint model. The result of the simulation of the hammer mechanism coupled with the bolted joint is then compared to the experimental data of the tightening process.

## 3 Results and discussion

This chapter describes the results and discussion of the conducted case study. Firstly, the results from the preliminary study as a basis for qualitative modeling are described. Then, the built-up C&C$^2$ sequence model is

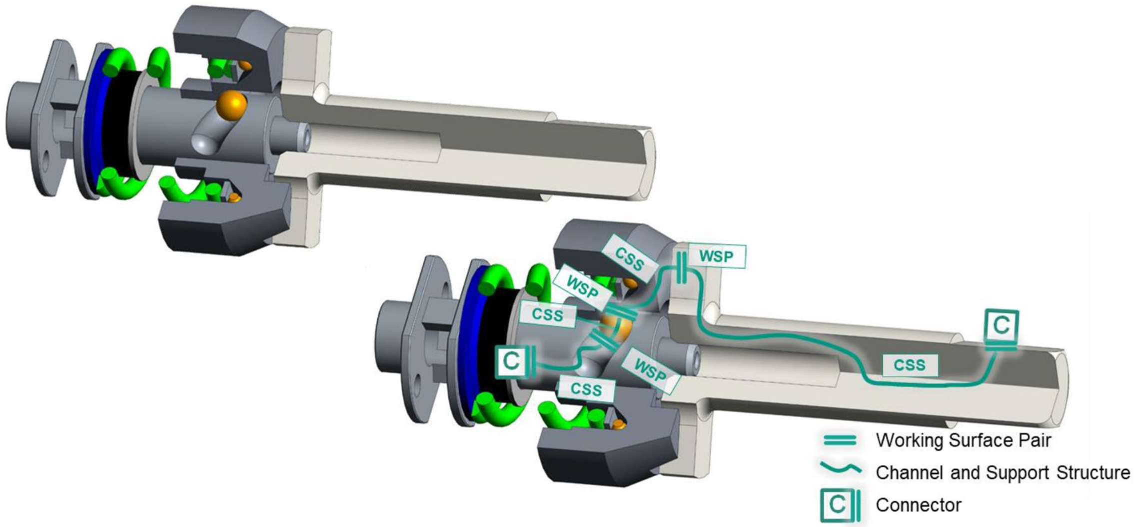

**Fig. 9** C&C$^2$-Model of the hammer mechanism of the impact wrench according to [16]

shown. Based on this model, parameter identification is dealt with, and finally, model validation against experimental data is described.

## 3.1 Modeling of embodiment function relations of the impact wrench

The following chapters describe qualitative modeling from its basis in the preliminary study to the definition of states, function-relevant elements, and parameters in the C&C$^2$-Sequence model. This model is then validated by parameter identification in a simulation model, where assumptions from the model are checked for their quantitative influence on the system behavior.

## 3.2 System structure model from the preliminary study

Figure 9 shows the initial C&C$^2$-Model of one state of the analysis. It shows the main channel and support structure and the working surface pairs, which are crucial for interactions in the hammer mechanism. On this basis, the state changes of the system are modeled.

At the overall system observation level, two operational states are differentiated for the described impact mechanism. A torque threshold functions as a trigger for those states (compare also Sect. 1.2). The system is in the first state when the demanded output torque is below this threshold. In this state, torque is transmitted at a nearly constant angular speed and the impact wrench works like an electric screwdriver. In the bolting application, this state is called 'run-down'. The system switches into the second operational state when the threshold is reached and the hammer mechanism is activated. While in this state, various sub-states emerge, where the system behavior varies greatly. This case study focuses on the second state and its sub-states.

Experimental investigations show that not always, a linear system behavior change occurs but depending on the parameters of the process, also different behaviors can emerge. Figure 10 shows, for example, a second force peak in the data that can occur depending on the parameters in the bolted joint and system dynamics. This means that not only one impact happens, as is expected, but also another one whose causes are unclear.

This behavior was previously investigated using a specially prepared power tool and a high-speed camera to observe the behavior of hammer and anvil (Fig. 10, left side) [16].

### 3.2.1 Building up the C&C$^2$-sequence model

The identified states of the system are investigated further, as a valid simulation model needs to consider this behavior as well. An overview of the resulting C&C$^2$-Sequence model derived from the gained insights is shown in Fig. 11.

This sequence model shows six states that can occur depending on the operating status of the impact wrench and the behavior of the bolted joint. The transitions between the States are modeled smooth with regard to their physical properties. The first state in this model is called spring relaxation. The hammer accelerates in positive angular direction due to the decompression of the previously compressed spring. The second state is reached when the acceleration of the hammer is finished. In this state, the hammer rotates at an approximately constant

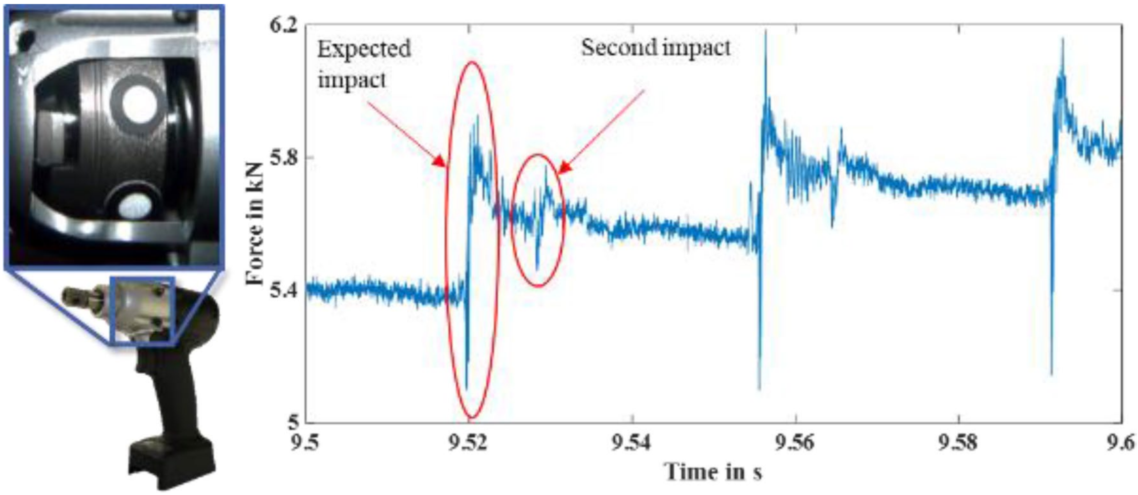

**Fig. 10** Phenomenon in the preload force of a screw connection fastened by the impact wrench [16]

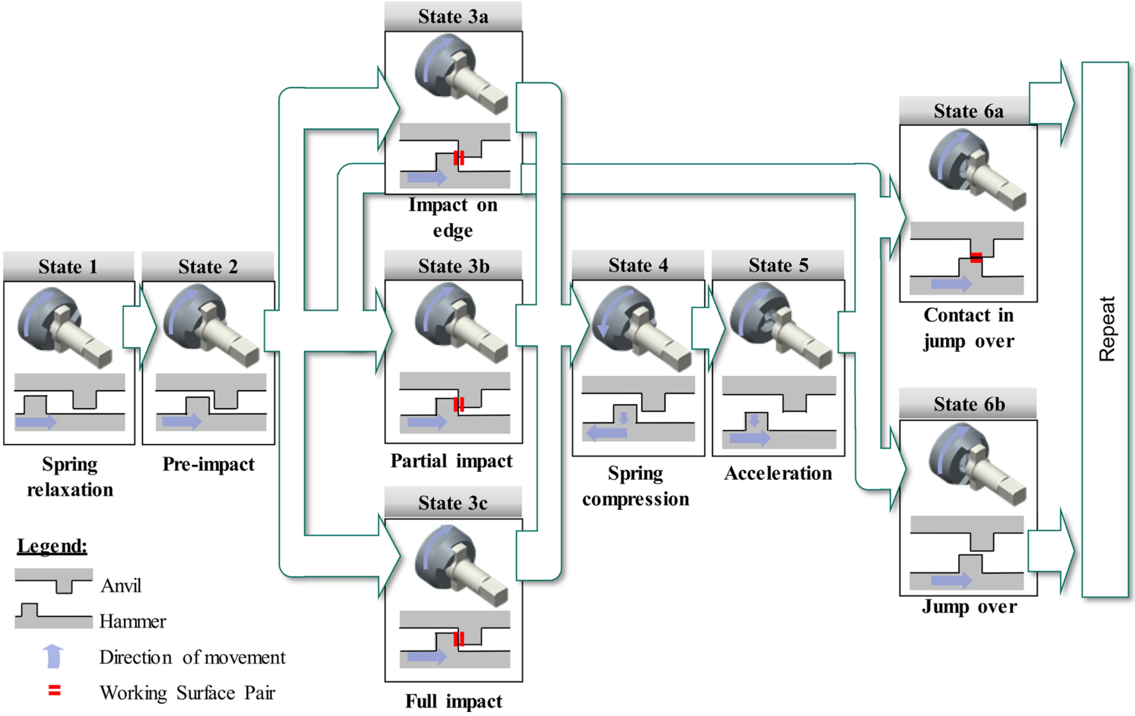

**Fig. 11** Simplified C&C$^2$-Sequence Model of the states of the activated hammer mechanism

speed. The third state shows the impact, where a tangential working surface pair between hammer and anvil emerges. In this state, the resulting tangential interaction between hammer and anvil creates the output torque with an impulse characteristic. The amplitude and duration of the impact torque depend on many parameters like the moment of inertia, the angular speed, system stiffness, and the interactions with the bolted joint.

In the model, three logical sub-states are differentiated for the impact. In state 3a, the hammer hits the edge of the anvil, in 3b, the anvil is hit partially, and in 3c, a full impact occurs. These three states also lead to different torque peaks. After that impact, the fourth state starts with disbanding of the working surface pair between hammer and anvil. The recoil reverses the angular hammer speed, which causes the axial movement of the hammer

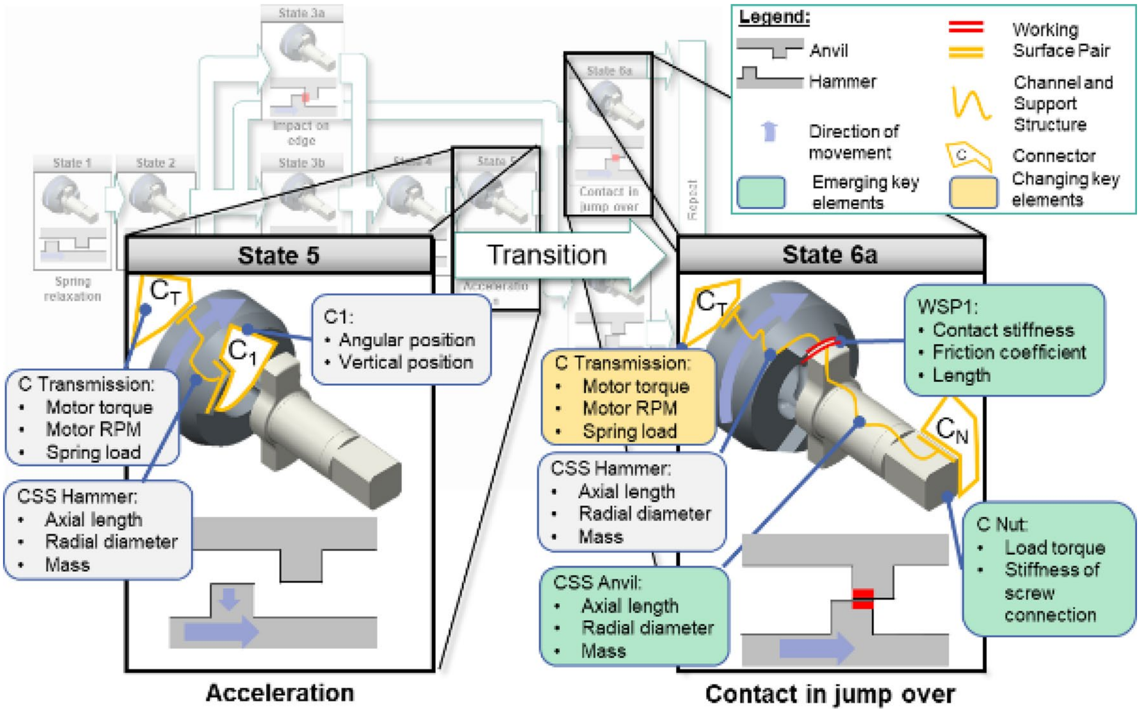

**Fig. 12** Exemplary parameters in the C&C$^2$-Sequence model of the hammer mechanism

and spring compression due to the interaction between the working surface pairs of the ball contact. In the fifth state, the hammer is accelerated again, while the spring is still compressed and therefore the hammer is also axially displaced. From the fifth state, it might also happen that another partial impact (state 3b) occurs. This can repeat depending on the process parameters until the spring has built up a pressure high enough to move the hammer over the anvil.

The sixth state can again be differentiated in two logical states that differ greatly in their behavior. In state 6a, the hammer jumps over the anvil and touches the upper side of the anvil, creating friction contact in the WSP. In 6b, the hammer jumps over the anvil without contact. After states 6a or 6b, the sequence is finished.

With the jump-over in states 6a or 6b, the spring starts to decompress and the sequence then starts again with the first state. Since the anvil and hammer each have two 180° offset striking surfaces, the sequence is repeated twice every 360° mechanical rotation of the drive shaft with fixed anvil. An excerpt of detailed models with parameters is shown in Fig. 12.

Here, states 5 and 6a are depicted. In state 5 *acceleration*, the movement of the hammer is in the focus of the modeling process. Influencing parameters on the acceleration of the hammer are, for example, the mass and radial diameter of the CSS hammer or the angular and vertical positions of the C1. In the transition to state 6a *contact in jump-over*, new key elements emerge (shown in green). C1 dissolves into WSP1 as the anvil becomes relevant to the system's behavior. Here, the contact stiffness, friction coefficient, and length are assumed to influence the system's behavior. Being connected to the WSP1, the CSS anvil also is modeled with its length and mass. The model ends with the Connector C nut, where the load torque and stiffness of the screw connection are assumed relevant.

Based on this model understanding, the simulation model is derived and implemented in Simscape™ following the states defined in the C&C$^2$-Sequence model. The states are not modeled as discrete states but as a continuous model, therefore the multibody library is used. Figure 13 shows the principal structure of the multibody model.

Whereas $J_m$, $J_h$, $J_{a1}$, and $J_{a2}$ denote the mass moments of inertia of the motor, the drive shaft, hammer, and anvil $c_{ms}$, $c_{ds}$, $c_s$, and $ca$ denote the damping coefficients of the motor shaft, the drive shaft, the spring, and the anvil. $k_{ms}$, $k_{ds}$, $k_s$, and $k_a$ denote the stiffness coefficients of the motor shaft, the drive shaft, the spring, and the anvil. $T_m$ is the torque delivered by the motor, and $T_{bh}$ the reaction torque of the bolt head. Besides, the shown parameters are additional parameters of the spring-groove mechanism and the impact contact.

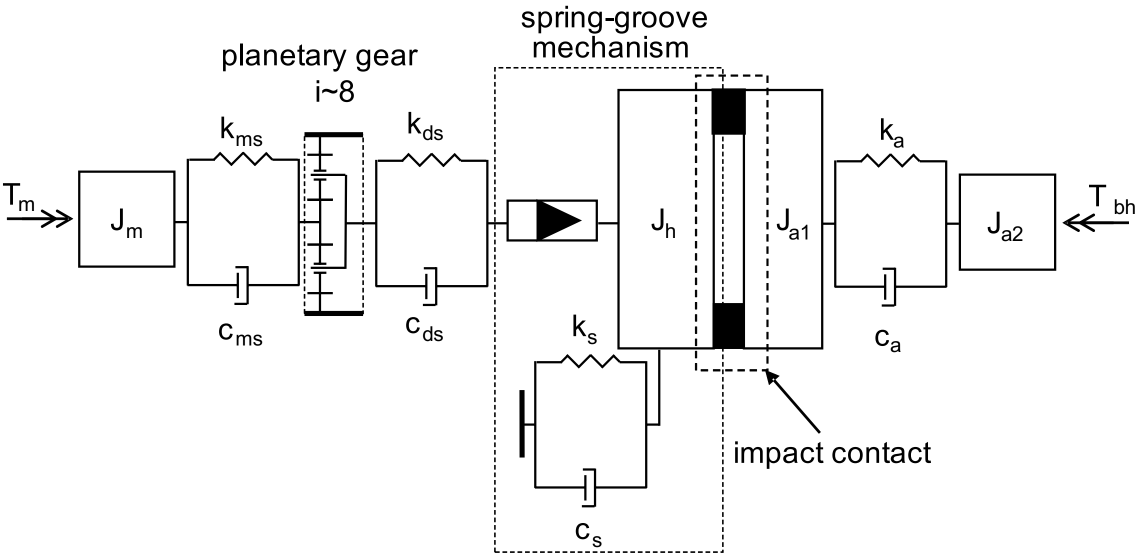

Fig. 13 Multibody model of the impact wrench

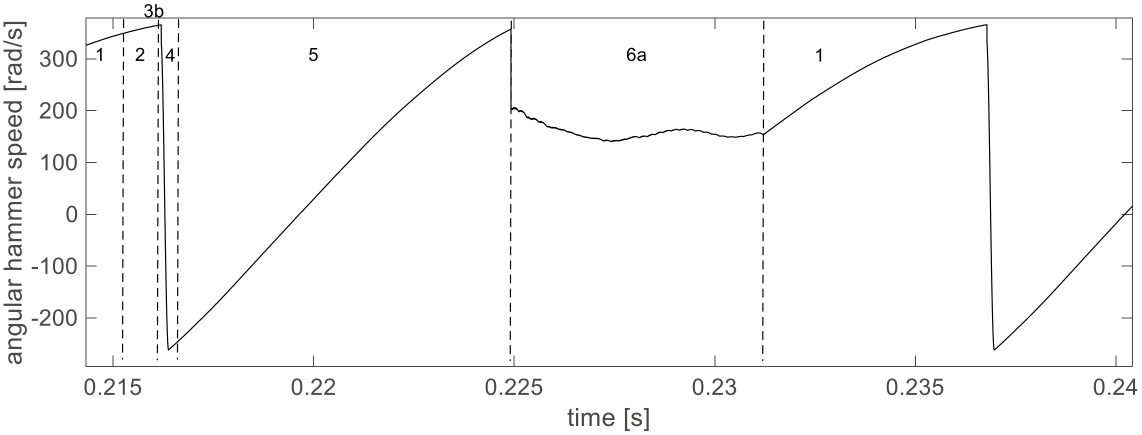

Fig. 14 angular hammer speed over time during one impact cycle

### 3.2.2 Parameterization through simulation

For parameterization, the states from the C&C$^2$-Sequence model are used together with the parameters in the key elements. The qualitative movement of the hammer mechanism shown in Fig. 12 creates the basis for the multibody model. Here, in state 5, the hammer mass is accelerated and in state 6a, the hammer mass jumps over the anvil sliding in contact. To parameterize the model in Fig. 14, the angular hammer speed over time is shown.

In the figure, the vertical lines divide the impact cycle into the states shown in the overview of the C&C$^2$-Sequence model in Fig. 11. Just after the impact and the spring compression in state 5, the spring decompresses and accelerates the hammer mass. The main parameters in that state are $k_s$ and $c_s$, but, as is shown by the C&C$^2$ Model of this state in Fig. 12c, they are not the only ones. Looking at the connector $C_T$, it can be seen that also the properties of the transmission and the motor affect the acceleration behavior. Although these properties also have an influence, this state should mainly be used to define $k_s$ and $c_s$, because to parameterize the properties of the transmission and the motor model, for example, the initial ramp- up sequence of the system can be used.

In the transition to state 6a, a new WSP emerges. Therefore, other parameters are the main parameters in this state. In particular, the length of WSP1 (see Fig. 12) together with the current speed of the drive shaft define

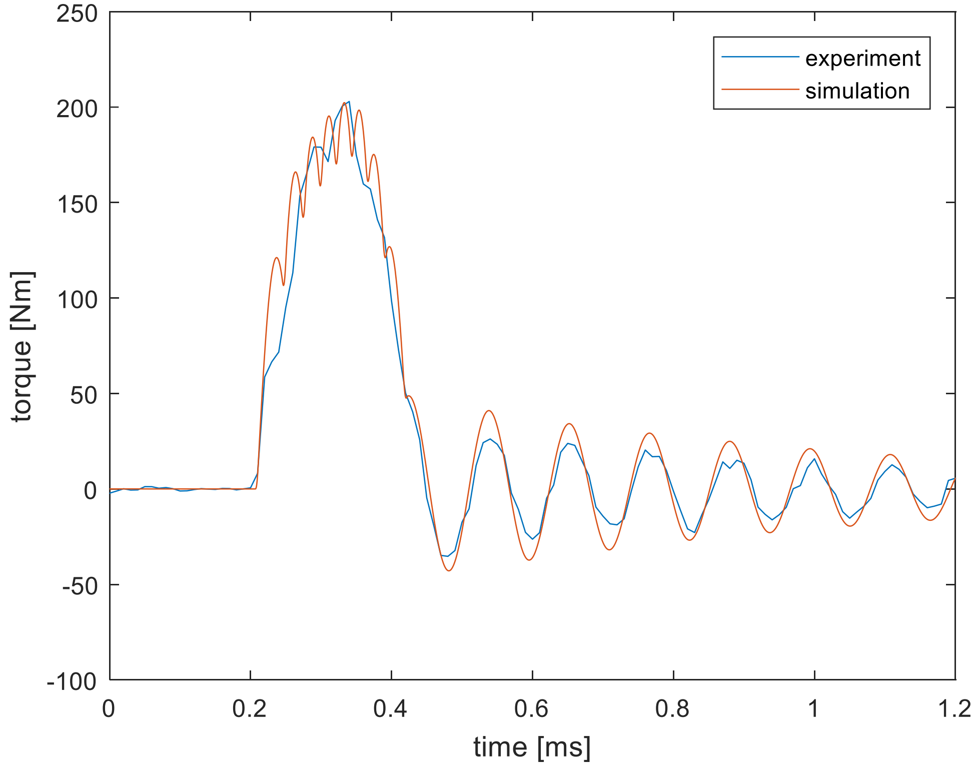

**Fig. 15** Impact torque of the hammer mechanism at a medium rotational speed after model parameter identification

the duration of the state, which itself is an important property since it also influences the following durations. Also, the vibration seen during that state reflects on several other parameters like the stiffness of the driving system, the spring, and the friction in WSP1 (see Fig. 12), which gives information which can be used for further parameterization.

During the parameterization process, assumptions regarding the underlying EFRs of the C&C$^2$-Sequence model were checked. Here, for example, it was found that the material damping as well as the frictional damping have a significant influence on the shape of the torque pulse. High damping to stiffness ratios lead to triangular pulses. Figure 15 shows the result of the parameterization. The measured data of the impact torque at a medium rotational speed was used for the iterative fitting of the simulation results to the experimental data. The test setup was modeled in the simulation and to obtain comparable results.

It can be seen that the impact duration and height of the computed data fit the experimental data well. Additionally, the shapes of the impulses seem to be very similar. Differences can be seen in the overlaying high-frequency vibration during the impact and in the abatement after the impact.

### 3.3 Experimental validation of the built-up simulation model

The validation of the hammer mechanism simulation model is based on experiments with different rotational speeds. For the three rotational speeds, three experiments were conducted. In total, more than 200 impacts per speed were measured, because the speeds differ and due to slightly different experiment lengths, the number of observations differs. Figure 16 shows exemplary results of the experiments in comparison to the simulation results, and Table 1 shows the means and standard deviation for the three speeds.

It can be seen that at both rotational speeds, the peak height and duration fit well, while the peak height varies between the three different speeds (compare Fig. 15). The abatement fits for the slow speed even better than for the medium speed (Fig. 15), while there is a discrepancy for the fast speed. The shape qualitatively fits the experimental data, too.

The next step in model validation is the comparison of the hammer mechanism coupled to a bolted joint model to experimental data. An experiment is conducted using the test setup described in Sect. 2.3. The measured coefficient of friction of the loosening process is used as a parameter in the bolted joint model. A value of $\mu = 0.0923$ was measured and used for the static as well as the sliding

**Fig. 16** Impact torque of the hammer mechanism at a slow (top) and fast (bottom) rotational speed

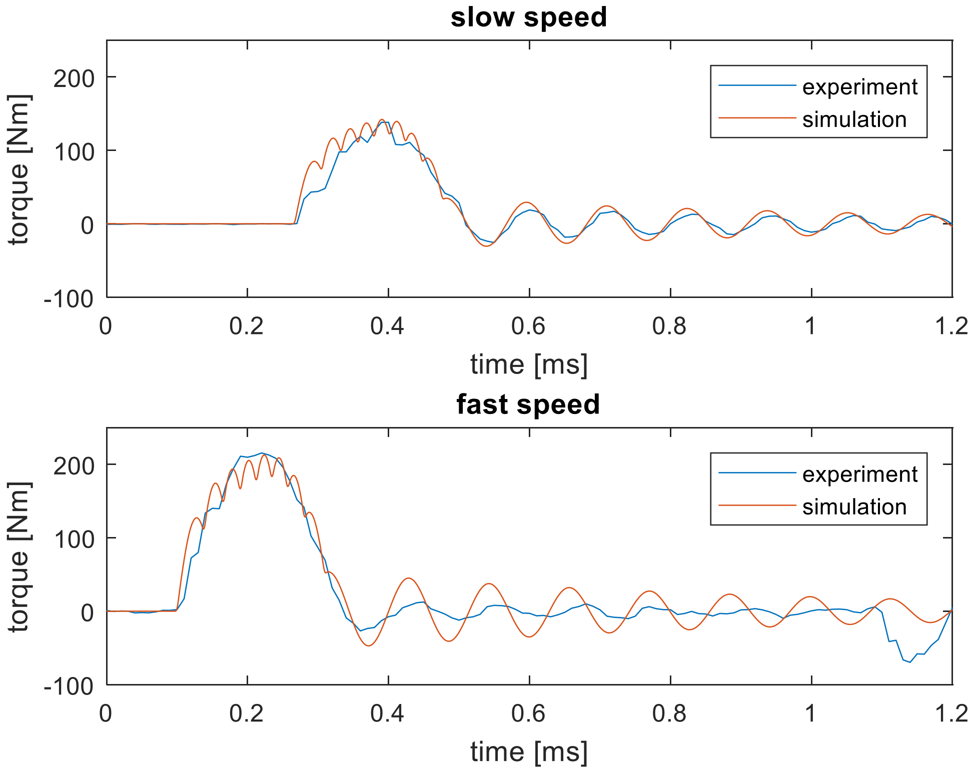

**Table 1** Means and standard deviations of the measured torque peaks at different speeds

| speed | Number of impacts [-] | Mean value [Nm] | Standard deviation [Nm] |
|---|---|---|---|
| slow | 366 | 115.5 | 10.6 |
| medium | 859 | 192.2 | 20.6 |
| high | 1016 | 209.0 | 26.1 |

friction. The velocity-dependent viscous component of the friction is used as a free parameter for simulation at the medium speed to consider the occurring sliding speeds between the frictional surfaces. It was determined to amount to 0.6 Nm/(rad/s). Figure 17 shows the comparison of the simulation with the experimental data based on the course of the preload force over time.

The time that is necessary to reach 25 kN is nearly the same for both results. Both curves show a logarithmic shape, whereas simulation starts slightly steeper and ends slightly steeper with a lower gradient. Whereas the slope of the preload force rises smoothly at the beginning, becomes higher, and becomes smoothly lower at the end again. Furthermore, it should be noted that the speed of rotation in the simulation is 25% lower than that in the experiment. This means that although the torque impulses have a lower height, they lead to a higher force increase in the simulation. Hence, the variation of the gradient in the experiment is more complex than represented in the model. To find a possible reason for this discrepancy in Fig. 18, a comparison of the dynamic thread torque between the experiment and the simulation is shown.

The plot shows that from the beginning of the process, the maxima of the thread torque in the experiments rise smoothly until they reach a steady level. Whereas in the simulation, the maxima of the thread torque are constantly high. The course of the static thread torque (mean value between impacts) in the simulation is very similar to the course revealed by the experiment.

## 4 Discussion

A structured qualitative parameterization with the C&C$^2$-Approach as a basis for the simulation model of the hammer mechanism support joint simulation with a bolted joint model. Consideration of the relevant parameters and necessary simplifications by aligning the simulation model to the C&C$^2$-Sequence model of the hammer mechanism was implemented. In the following iterative parameterization of the simulation model, targeted adjustments to the parameter values were possible. In this process, indications for true as well as for false EFRs were collected and thus, additional system knowledge was built.

Due to the parameterization based on the EFRs, the results of the model validation show a broad range

**Fig. 17** Comparison of experimental and computed data at the medium speed level

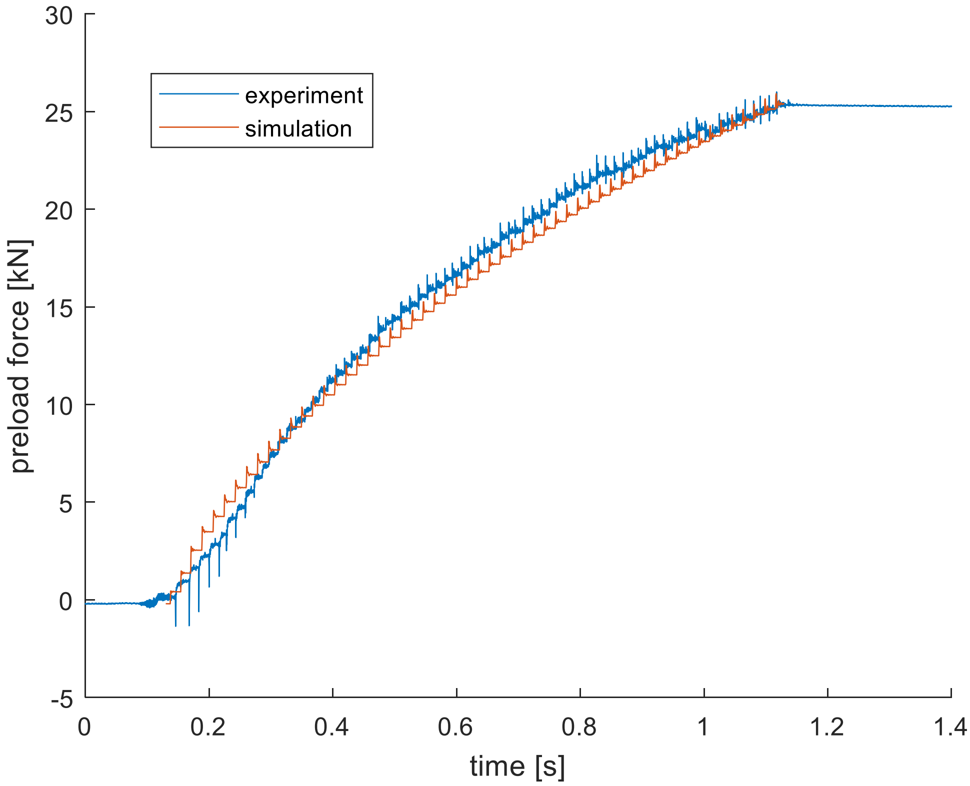

**Fig. 18** Comparison of experimental and computed thread torques during tightening of a bolted joint with an impact wrench

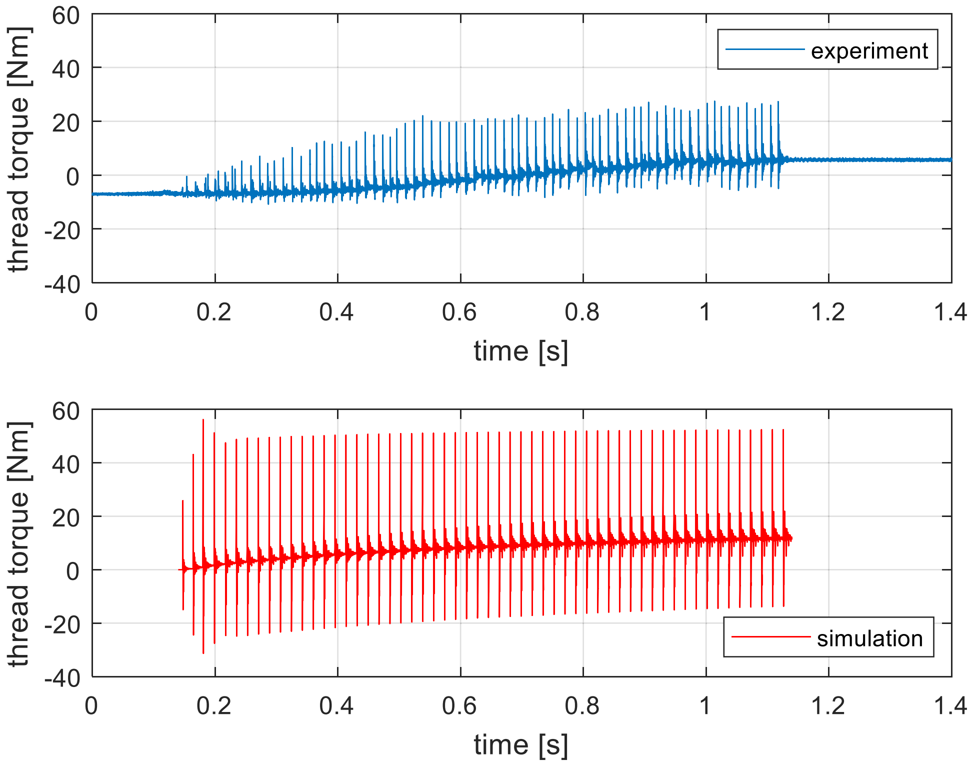

of validity in relation to the rotational speed, which is shown in Fig. 16. The coupling of the hammer mechanism model with the bolted-joint model lead to a good result during application of the preload force, see Fig. 17, which indicates a good model quality and shows that the right parameters were chosen. The stated differences between the simulation and the experiment can be unraveled to issues in the representation of the embodiment and its behavior. For example, the smoother increase in preload force in the experiment might be due to the alignment between the WSPs perpendicular to the preload force, which is not represented in the model. Another aspect was shown by the measured deviation in the course of thread friction. Therefore, it might be stated that the model needs to be refined to better represent the interactions in the WSP in the bolted joint. A correct representation of the WSP interactions is required to be able to describe the EFRs in the whole system model.

In contrast to other research work using, for example, multi-objective algorithms for parameter identification [24], the C&C$^2$-Sequence model is used for parameter identification. Thus, the approach connects qualitative results on the EFR of the analysis with the simulation model.

The qualitative definition of system states through the C&C$^2$-Sequence model enabled a structured parameterization of the simulation model, as the system analysis could be focused on single states instead of considering the whole sequence. When the unknown system behavior was identified, the C&C$^2$-Sequence model was extended and the additional states could be integrated into the simulation.

In this case study, the hammer mechanism model was parameterized using the medium rotational speed. The simulation results were valid for the two other rotational speeds, regarding peak height and duration, as well as the simulation together with the coupled bolted joint model. This indicates a broad validity range of the model based on the detailed insights into the causes of the system's behavior. However, as this was not in the focus of the investigation, no statement is possible as to whether this validity range could also have been reached using different approaches. During the modeling process, many insights were implemented into the simulation model and can be traced back to assumptions made in qualitative modeling. Therefore, it can be stated that this modeling approach is suitable for modeling systems with complex dynamic behavior. However, this statement is based only on the investigation of the impact wrench. Transferability has to be investigated for other cases of dynamic systems modeling.

While modeling states of a dynamic system, a limitation of the C&C$^2$-Approach was identified, as the states mostly did not change through emerging or disbanding key elements but through massive changes of their properties, such as moving direction, acceleration, etc. Emerging and disbanding key elements can be displayed clearly, however, there are no defined elements to visualize changing of the properties, especially if the properties are state-bound. The colored arrows are used often (see also [12]), however they are not defined in the C&C$^2$-Approach.

## 5 Conclusion

The parameterization of a simulation model through qualitative modeling of EFRs by using the C&C$^2$ Approach supported in the conducted case study in system analysis of the dynamic behavior of an impact wrench. Qualitative modeling supported parameter identification through visualization of the system's EFRs and enabled the trace-back of parameters to assumptions made by the design engineers in model building.

With the simulation model, the real dynamic system behavior was modeled with an initial sufficient precision. Weaknesses in the frictional behavior were found and possible causes in the system's embodiment were assigned using the C&C$^2$-Model. Future research will address these model issues. To improve modeling of the impact mechanism, a parameter study based on Design of Experiment might be conducted. On this basis, the range of application for impact wrenches might be increased someday through better prediction of the preload force of a bolted joint based on simulation models of the power tool and its environment. A limitation of the C&C$^2$-Approach in modeling changes of properties has been discovered, which creates potential for further research into modeling of dynamic system behavior. As the results of this research are based on a case study, generalized statements are difficult to derive. For improvement of the external validity of the structured approach, investigation of other dynamic systems is required. To improve the internal validity and identify causal relations, this approach needs to be transferred into a controllable investigation environment. The development of this environment is a major challenge, as a close-to-reality development scenario has to be broken down into manageable parts that enable purposeful investigation. This challenge will be addressed in the future.

**Funding** Open Access funding enabled and organized by Projekt DEAL.

### Compliance with ethical standards

**Conflict of interest** The authors declare that there is no conflict of interest.

## References

1. Suh NP (1998) Axiomatic design theory for systems. Res Eng Des 10(4):189–209
2. Gero JS, Kannengiesser U (2004) The situated function-behaviour-structure framework. Des Stud 25(4):373–391
3. Weber C (2005) CPM/PDD-an extended theoretical approach to modelling products and product development processes. Ger-Isr Symp 2:159–179
4. Weber C (2014) Modelling products and product development based on characteristics and properties. In: Chakrabarti A, Blessing LTM (eds) An Anthology of Theories and Models of Design: Philosophy, Approaches and Empirical Explorations. Springer, London, London, pp 327–352
5. Stylianou DA (2002) On the interaction of visualization and analysis: the negotiation of a visual representation in expert problem solving. J Math Behav 21(3):303–317
6. Andreasen MM, Hansen CT, Cash P (2015) Conceptual design: interpretations, mindset and models. Springer International Publishing, Cham, Switzerland
7. Chen PP-S (1976) The entity-relationship model-toward a unified view of data. ACM Trans Database Syst 1(1):9–36
8. Harel D (1987) Statecharts: a visual formalism for complex systems. Sci Comput Program 8(3):231–274
9. Yildirim U, Campean F, Williams H (2017) Function modeling using the system state flow diagram. AIEDAM 31(4):413–435. https://doi.org/10.1017/S0890060417000294
10. Gericke K, Eisenbart B (2017) The integrated function modeling framework and its relation to function structures. AIEDAM 31(4):436–457. https://doi.org/10.1017/S089006041700049X
11. Mokhtarian H, Coatanéa E, Paris H (2017) Function modeling combined with physics-based reasoning for assessing design options and supporting innovative ideation. AIEDAM 31(4):476–500. https://doi.org/10.1017/S0890060417000403
12. Albers A, Wintergerst E (2014) "The contact and channel approach (C&C$^2$-A) - relating a system's physical structure to its functionality", in *an anthology of theories and models of design: philosophy*. Springer, Approaches and Empirical Explorations, London, pp 151–171
13. Matthiesen S, Grauberger P, Sturm C, Steck M (2018) "From reality to simulation – using the C&C$^2$-approach to support the modelling of a dynamic system", in *28th CIRP design conference*. Nantes, France
14. Grauberger P, Wessels H, Gladysz B, Bursac N, Matthiesen S, Albers A (2020) The contact and channel approach – 20 years of application experience in product engineering. J Eng Des 31(5):241–265. https://doi.org/10.1080/09544828.2019.1699035
15. Matthiesen S, Grauberger P, Schrempp L (2019) "Extended Sequence Modelling in Design Engineering – Gaining and Documenting Knowledge about Embodiment Function Relations with the C&C$^2$-Approach," in *Proceedings of the 22nd International Conference on Engineering Design ICED19*, Delft, The Netherlands
16. S Matthiesen, A Wettstein, P Grauberger (2018) "Analysis of dynamic system behaviour using sequence modelling with the C&C$^2$-Approach – a case study on a power tool hammer mechanism," in *Proceedings of the NordDesign 2018*, Linköping, Sweden
17. VDI 3822 (2011) Schadensanalyse - Grundlagen und Durchführung einer Schadensanalyse
18. Ehrlenspiel K, Meerkamm H (2017) Integrierte Produktentwicklung: Denkabläufe, Methodeneinsatz, Zusammenarbeit, 6th edn. Carl Hanser Verlag GmbH & Co. KG, München, Wien
19. Matthiesen S, Mangold S, Bruchmueller T (2018) The influence of variating passive user interactions on power tools in the context of product development. Forsch Ingenieurwes 82(2):157–168. https://doi.org/10.1007/s10010-018-0269-x
20. Sieling P (1977) Untersuchungen zum Drehschlagschrauben. VS Verlag für Sozialwissenschaften, Wiesbaden
21. VDI 2230 (2015) Systematische Berechnung hochbeanspruchter Schraubenverbindungen Zylindrische Einschraubenverbindungen., 2230
22. Wallace P (2015) "Energy, torque, and dynamics in impact wrench tightening" transactions of the ASME. J Manuf Sci Eng 137(2):024503/1-024503/8. https://doi.org/10.1115/1.4028750
23. T Bruchmueller et al. (2015) "An Adjustable Impedance Element – System Requirements and Design Approach," in *Proceedings of the 26th Symposium Design for X*: TuTech Verlag, Hamburg
24. Zhang S, Tang J (2016) System-level modeling and parametric identification of electric impact wrench. J Manuf Sci Eng 138(11):111010/1-111010/16. https://doi.org/10.1115/1.4033044
25. Japing A, Seibel A, Schlattmann J (2015) "Modellentwicklung zur Beschreibung von Reibschwingungen bei der Schraubenmontage," in *Reibung, Schmierung und Verschleiß: Forschung und praktische Anwendungen, Tribologie-Fachtagung, 56*, Aachen: GfT, 2015, 63/1–63/10
26. Croccolo D, de Agostinis M, Vincenzi N (2012) Influence of tightening procedures and lubrication conditions on titanium screw joints for lightweight applications. Tribol Int 55:68–76. https://doi.org/10.1016/j.triboint.2012.05.010
27. Espinosa HD, Patanella AJ, Fischer M (2000) Dynamic friction measurements at sliding velocities representative of high-speed machining processes. J Tribol 122(4):834–848. https://doi.org/10.1115/1.1310331
28. Matthiesen S, Wettstein A, Sturm C (2018) "Eine qualitative Untersuchung der Reibungsverhältnisse und des Oberflächenverschleißes in schlagend angezogenen Schraubenverbindungen", in *Schraubenverbindungen 2018*. Würzburg, Germany
29. DIN, "DIN EN ISO 16047: Verbindungselemente - Drehmoment/Vorspannkraft-Versuch (ISO 16047:2005 + Amd 1:2012); Deutsche Fassung EN ISO 16047:2005 + A1:2012," vol. 2012, 2012
30. IPEK, "IPEK Inside," 2018. [Online]. Available: http://www.ipek.kit.edu/downloads/IPEK_inside_2018_p.pdf. accessed 07.11.2019